

# A Study of the Machinability of Metals

(Effect of microstructure on cutting mechanism,  
tool life, and surface finish)

By

Keiji OKUSHIMA and Kazuaki IWATA

(Received October 26, 1962)

The effect of microstructure of materials on machinability of carbon steels (S15C, S40C and SK4) was investigated from the viewpoint of cutting mechanism, tool life, and surface finish.

The experimental results on cutting mechanism are studied in the first half of this paper.

It was found that inclination angle of the starting boundary line of the flow region was almost constant, and inclination angle of the end boundary line and the size of the flow region showed a maximum value at the lamellar portion of pearlite of 20-30%.

The results obtained from the experiments on tool life and surface finish are studied in detail in the later half of this paper.

The effect of spheroidized pearlite structure in high carbon steels on machinability was compared with the lamellar pearlite structure.

## 1. Introduction

The various problems on the machinability of metals have been studied and considerable effort has been made recently to systematize the machinability evaluation made by many researchers.

At the present stage of the field of metal cutting machinability of metals is evaluated by means of tool life, surface finish, consumption power (cutting force), chip control, and so on.

It appears that theoretical and experimental analysis about the various factors influencing the machinability (i.e., chemical properties, microstructure, and heat treatment, etc.) are necessary for this research.

In this paper, the effect of microstructure on machinability was investigated. The materials tested were three grades of carbon steel (S15C, S40C, and SK4) containing four different kinds of lamellar pearlite microstructure and one grade of high carbon steel consisting of spheroidized pearlite structure.

## 2. The properties of materials tested and experimental procedures

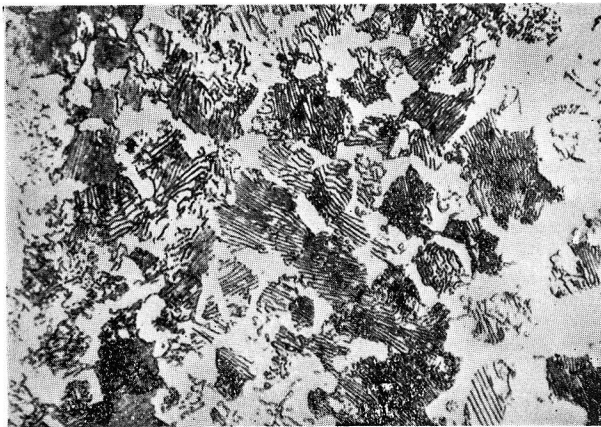
Regarding the four kinds of carbon steel tested, the lamellar portion of pearlite was 90-100, 50-60, 20-30, and 0-10 per cent.

The chemical compositions and Brinell hardness of these materials are shown in Table 1 and typical microphotographs are shown in Fig. 1.

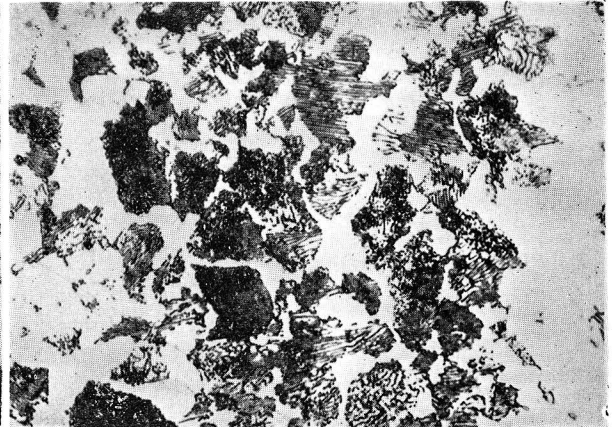
Chemical composition \ Work material	C	Si	Mn	P	S	Cu	Ni	Cr
SK 4	0.99	0.19	0.37	0.018	0.011	0.19	0.08	0.10
S 40 C	0.41	0.22	0.70	0.024	0.010	0.26	0.11	0.20
S 15 C	0.17	0.23	0.36	0.008	0.016	0.15	0.09	0.07

Work material \ Lamellar portion of pearlite (%)	S 15 C	S 40 C	SK 4
90~100	119	169	229
50~60	120	179	223
20~30	130	201	293
0~10	131	201	293

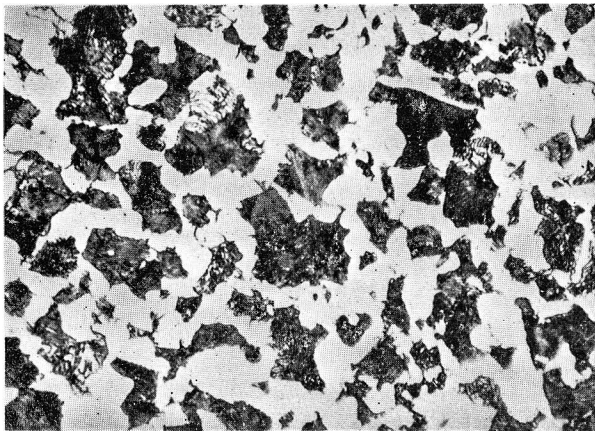
Table 1.  
The chemical compositions and Brinell hardness of Work Materials



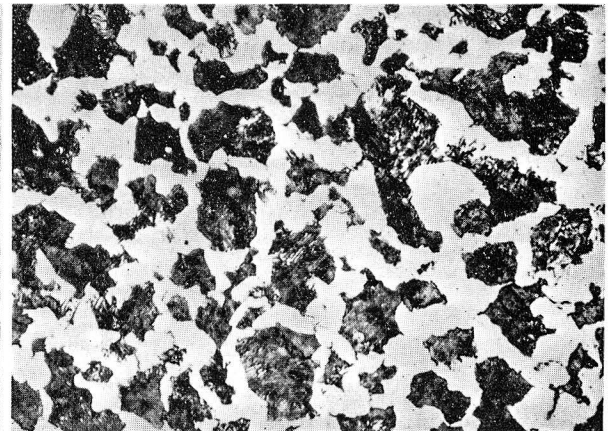
(a) lamellar portion of pearlite of 90~100%



(b) lamellar portion of pearlite of 50~60%



(c) lamellar portion of pearlite of 20~30%



(d) lamellar portion of pearlite of 0~10%

Fig. 1. Typical microphotograph of work materials (S40C)

(×500)

Brinall hardness decreases with an increase in the lamellar portion of pearlite. This tendency is evident for high carbon content in steel.

Cutting tests were carried out dry in a high speed lathe (Niigata Iron Works Co ; swing, 500 mm ; power, 15 HP).

The cutting tool used was of steel cutting grade carbide P-10 (ISO). Tool geometry and feed were varied as follows.

(a) Orthogonal cutting for analysis of cutting mechanism

Tool geometry ;

Back rake angle	0 deg.
Side rake angle	5 deg.
End relief angle	5 deg.
Side relief angle	5 deg.
End cutting edge angle	5 deg.
Side cutting edge angle	0 deg.
Nose radius	0.1 mm

Feed ; 0.1, 0.18, 0.28 and 0.40 mm/rev.

(b) Conventional cutting for tests of tool life and surface finish

Tool geometry ;

Back rake angle	0 deg.
Side rake angle	5 deg.
End relief angle	5 deg.
Side relief angle	5 deg.
End cutting edge angle	15 deg.
Side cutting edge angle	15 deg.
Nose radius	0.3 mm

Feed ; 0.18, 0.28 and 0.40 mm/rev. for tool life tests

0.06, 0.18 and 0.28 mm/rev. for surface finish tests

Tool forces were measured with a three-component tool dynamometer of the strain gage type<sup>1)</sup>. A needle type optical roughness meter was used to measure the surface finish.

### 3. Machinability evaluation from the standpoint of cutting mechanism

#### 3.1. Theoretical analysis of orthogonal cutting based upon the flow region concept

The cutting mechanism of lamellar pearlite microstructure of carbon steels was analysed based upon the flow region concept.

In this concept, theoretical equations for the cutting mechanism was deduced as follows<sup>2),3)</sup> ;

$$\phi_1 = \frac{1}{2} (K_1 - \beta + \alpha) \dots\dots\dots (1)$$

$$\phi_2 = \frac{1}{2} (K_2 - \beta + 2\alpha) \dots\dots\dots (2)$$

$$K_1 = \sin^{-1} \left\{ \frac{2}{k_1} \sin \beta + \sin (\beta - \alpha) \right\} \dots\dots\dots (3)$$

$$K_2 = \cos^{-1} \left\{ \frac{2}{k_2} \sin \beta - \cos \beta \right\} \dots\dots\dots (4)$$

$$k_1 = \frac{l}{t_1}, \quad k_2 = \frac{l}{t_2} \dots\dots\dots (5)$$

$$\Phi = \phi_2 - \phi_1 = \frac{1}{2} (\alpha - K_1 + K_2) \dots\dots\dots (6)$$

$$\tau_1 = \frac{(F_H \cos \phi_1 - F_V \sin \phi_1) \sin \phi_1}{bt_1} \dots\dots\dots (7)$$

$$\tau_2 = \frac{(F_H \cos \phi_2 - F_V \sin \phi_2) \cos (\phi_2 - \alpha)}{bt_2} \dots\dots\dots (8)$$

$$\gamma_2 = \cot \phi_2 + \tan (\phi_2 - \alpha) \dots\dots\dots (9)$$

$$\beta = \tan^{-1} \left\{ \frac{F_V + F_H \tan \alpha}{F_H - F_V \tan \alpha} \right\} \dots\dots\dots (10)$$

where  $\phi_1$  is inclination angle of the starting boundary line of the flow region,  
 $\phi_2$  is inclination angle of the end boundary line of the flow region,  
 $\Phi$  is sector angle of the flow region,  
 $\alpha$  is rake angle,  
 $\beta$  is mean friction angle,  
 $l$  is chip contact length,  
 $t_1$  is depth of cut,  
 $t_2$  is thickness of chip,  
 $\gamma_2$  is shear strain,  
 $\tau_1, \tau_2$  is shear stresses of the starting and end boundary lines of the flow region,  
 $F_H, F_V$  is principal and thrust cutting forces,  
 $b$  is width of cut.

**3.2. Experimental results and discussion**

The cutting force (principal and thrust cutting components), thickness of chip, and tool chip contact length were measured for various feed and rake angle when cutting lamellar pearlite materials. Using these experimental data, various important angle and stresses for analysis of cutting process were calculated from the above equations and are shown in Fig. 2 (a), (b), (c) and Fig. 3 (a), (b), (c) in relation to feed and rake angle.

**3.2.1. The effect of feed**

The variations of  $\phi_1, \phi_2, \Phi, \phi_0, \beta$ , are shown in Fig. 2 when the feed was

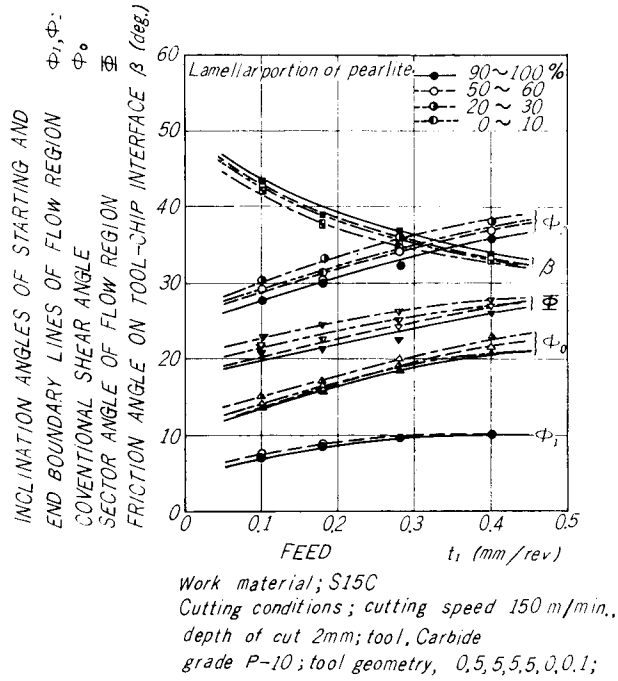


Fig. 2(a). Calculation value of low carbon steel (S15C) with feed.

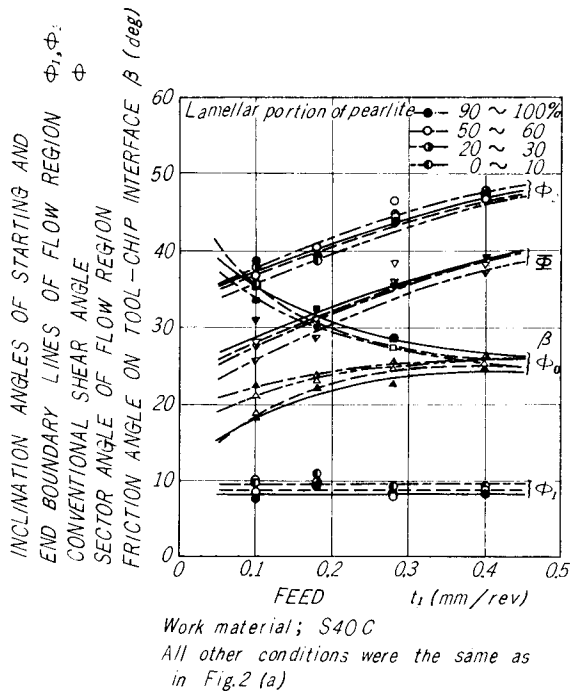


Fig. 2(b). Calculation value of medium carbon steel (S40C) with feed,

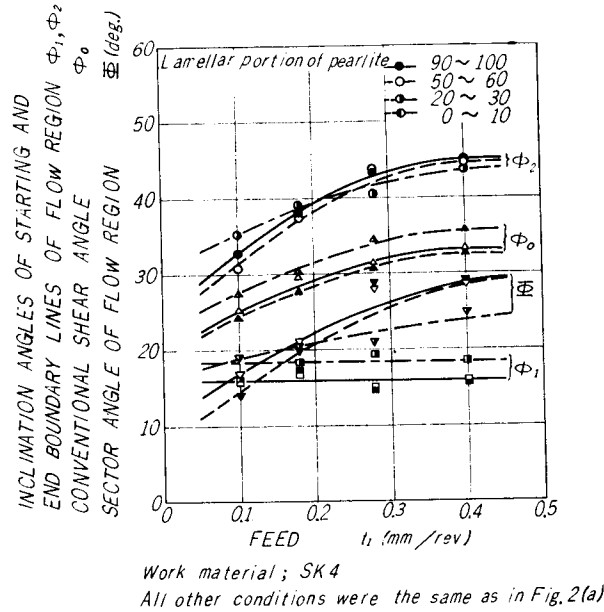


Fig. 2(c). Calculation value of high carbon steel (SK4) with feed.

varied as 0.10, 0.18, 0.28 and 0.40 mm/rev. for the cutting speed of 150 m/min, and the depth of cut of 2 mm constant.

It was found that with an increase in feed  $\phi_2$ ,  $\Phi$ ,  $\phi_0$  increases and  $\beta$  decreases for all grades of carbon steel.

This inclination was obvious when the feed was small. Finally, these values approached some constant values with an increase in feed.

This tendency was the same as in the case of alloy steel as we have already reported<sup>4)</sup>. Therefore, it is considered that this tendency is a common property for all kinds of steel.

$\phi_1$  was nearly constant in spite of variation in feed except for the S15C in which  $\phi_1$  increased gradually.

### 3.2.2. The effect of side rake angle

Similar calculated values when varying side rake angle as  $-20$ ,  $-10$ ,  $0$ ,  $10$ ,  $20$  deg. are shown in Fig. 3.

It is evident that  $\phi_1$ ,  $\phi_2$ ,  $\Phi$ ,  $\phi_0$ , and  $\beta$  increase with a decrease in side rake angle. Especially, the friction angle on tool face increases rapidly.

### 3.2.3. The effect of the lamellar portion of pearlite

#### (a) Cutting force (Principal and thrust components)

The relationship between microstructure and cutting force for the cutting

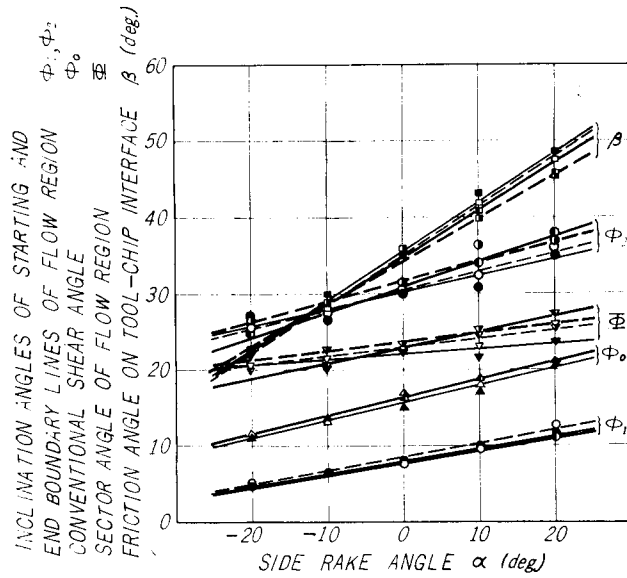


Fig. 3(a). Calculation value of low carbon steel (S15C) with side rake angle.

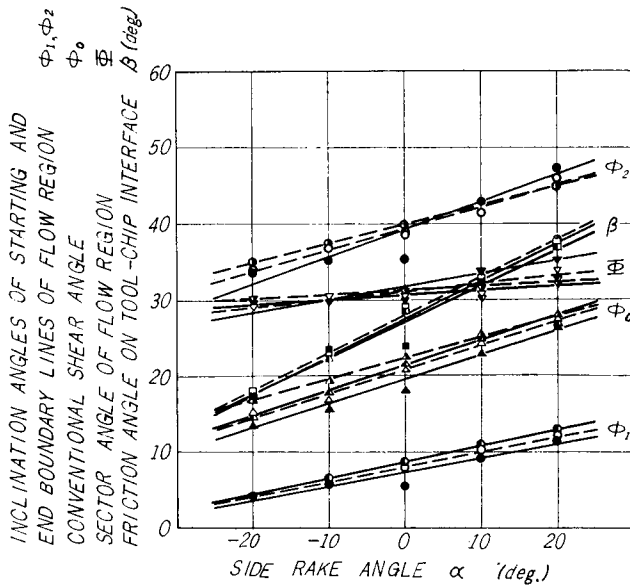


Fig. 3(b). Calculation value of medium carbon steel (S40C) with side rake angle.

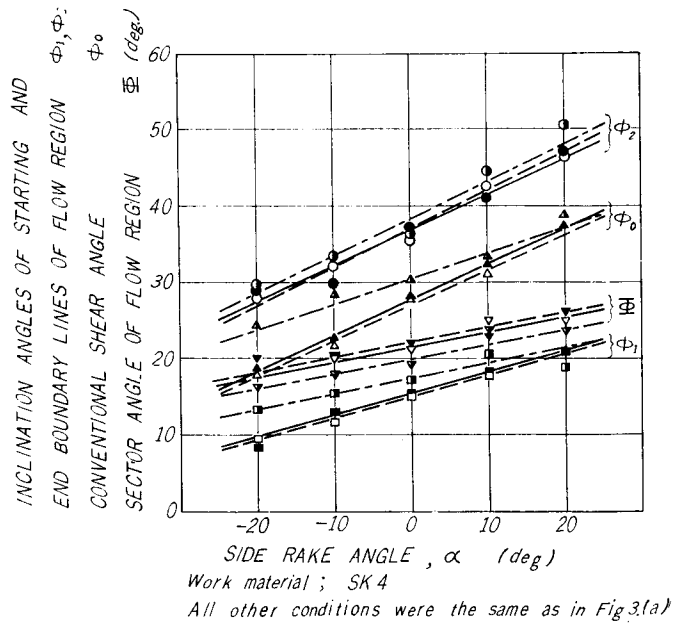


Fig. 3(c). Calculation value of high carbon steel (SK4) with side rake angle.

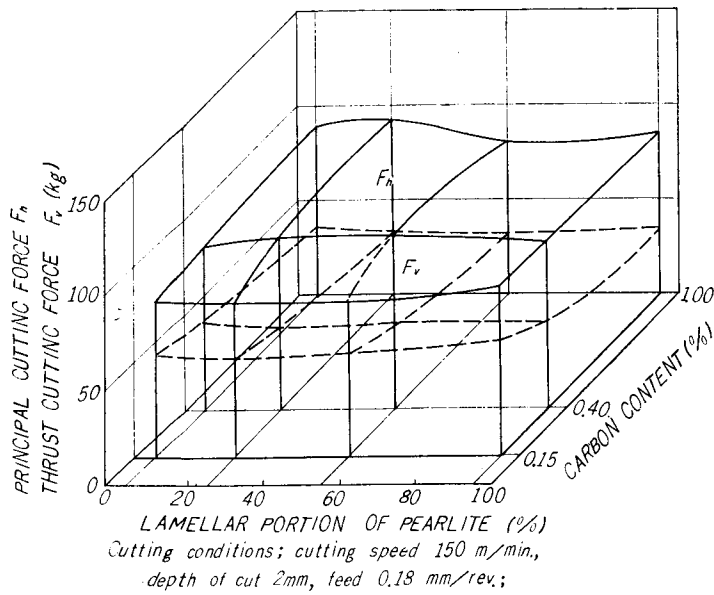


Fig. 4. Effect of microstructure (lamellar portion of pearlite) on cutting force,



speed of 150 m/min. and the depth of cut of 2 mm constant is shown in Fig. 4.

It was found that in the case of low carbon steel (S15C), the principal force increases with an increase of lamellar portion of pearlite. In the case of medium carbon steel (S40C), the principal force was maximum for the lamellar portion of 50-60%. This force value was about 6% larger than that for the lamellar portion of pearlite of 0-10%. However, the thrust force was almost constant. In the case of high carbon steel (SK4), the principal force reached the maximum value for the lamellar portion of about 20-30% and this value was about 14% smaller than that for the lamellar portion of pearlite of 50-60%. The thrust force was maximum for the lamellar portion of pearlite of 50-60%. This value was about 12% larger than the minimum value.

As mentioned above, the effect of microstructure differed for different carbon content when the lamellar portion of pearlite was varied. This is considered as follows: high carbon steel contains much carbide in its microstructure so that the Brinell hardness of the structure increases. Therefore, the decrease of the hardness by the lamination of the pearlitic structure results on of the decrease of cutting force.

The result of the hardness variation by varying pearlitic structure is shown in Table 2. The hardness of the portion of pearlite decreased with an increase in lamellar portion of pearlite.

Table 2.

Lamellar portion of pearlite (%)	0~10	20~30	50~60	90~100
Hardness	327	317	239	248

Low carbon steel contains much ferrite components and little carbide in its microstructure. The ferrite is generally sticky and difficult to machine.

Therefore, softening the carbide of small amount in low carbon steel by lamination increases the above mentioned tendency and results in an increase in cutting force.

Judging from the above mentioned phenomena, an increase in the lamellar portion of pearlite is effective in decreasing the cutting force for high carbon steel and not for low carbon steel. Besides, it appears that in the case of medium carbon steel the lamination of pearlite has little affect on cutting force, and so the machinability of medium carbon steel should be evaluated from the standpoint of tool life and surface finish.

(b) Conventional shear angle  $\phi_0$  and mean friction angle on tool face  $\beta$

Fig. 5 shows conventional shear angle  $\phi_0$  and mean friction angle on tool

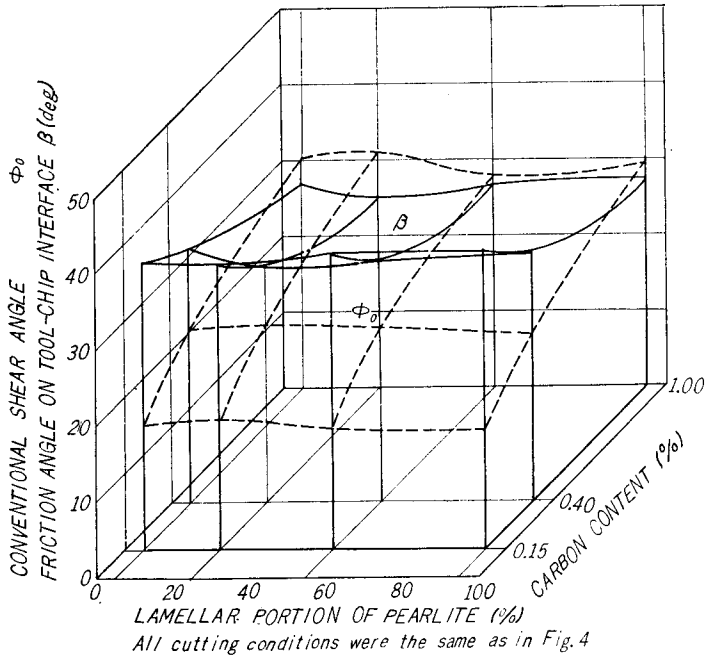


Fig. 5. Effect of microstructure (lamellar portion of pearlite) on conventional shear angle and friction angle on tool-chip interface.

face  $\beta$  in relation to the variation of the microstructure.

It was found that the conventional shear angle  $\phi_0$  increased with an increase in carbon content but the effect of variation of the lamellar portion in pearlite is little for low and medium carbon steels and much for high carbon steel.

On the other hand, the mean friction angle on tool face  $\beta$  shows a tendency to decrease with a decrease in the lamellar portion of pearlite. The higher the carbon content, the more considerable the effect of variation in pearlite microstructure.

#### 3.2.4. The effect of pearlite microstructure on shear stress and shear strain

The calculated values for shear stress on the flow region  $\tau_1$ , and conventional shear stress  $\tau_0$  are shown in Fig. 6.

Regarding the effect of the microstructure, it was observed that the shear stress decreases with an increase in the lamellar portion of pearlite.

In other words, the larger the lamellar portion of pearlite, the better the tool life.

Fig. 7 shows the shear stress on the flow region in relation to carbon content. The shear stress increased with an increase in carbon content in this experiment. The smaller the feed, the larger the shear stress. It appears that

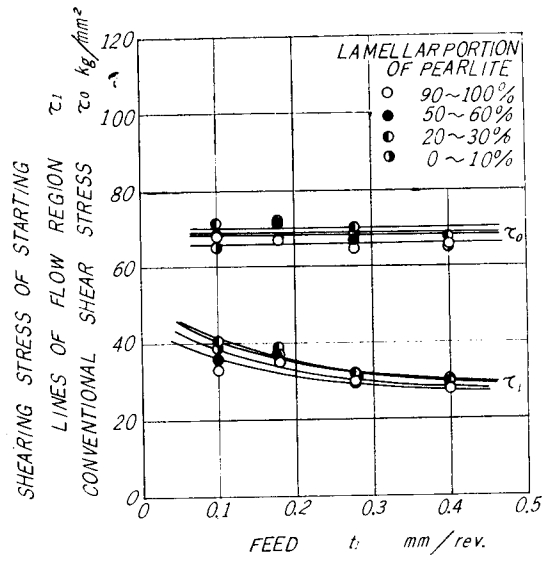


Fig. 6. Calculation value of medium carbon steel (S40C) with feed.  
All other conditions were the same as in Fig. 2(a).

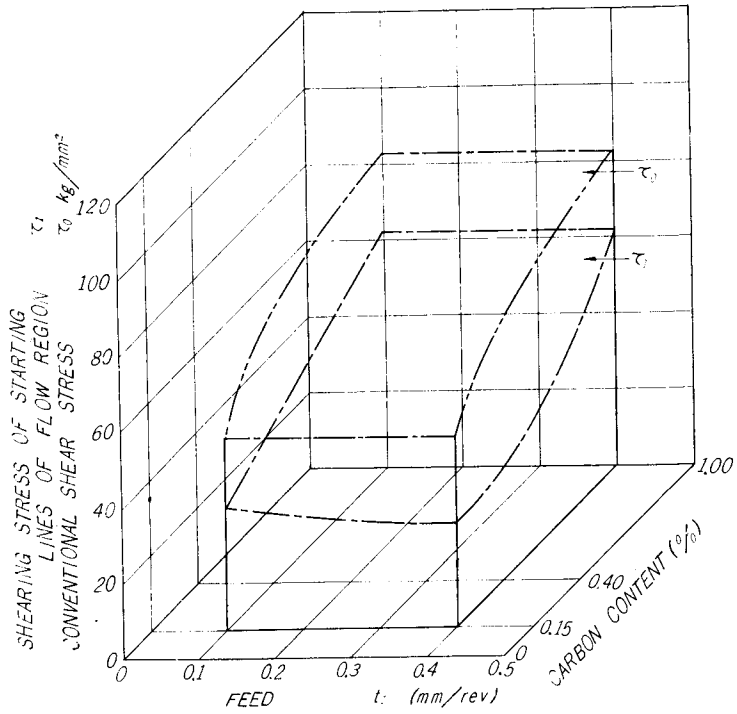


Fig. 7. Variation of shear stress with carbon content in steels and feed.  
All other conditions were the same as in Fig. 2(a).

the shear stress decreased with an increase in feed, because it is considered that the cutting temperature generally increases with an increase in feed so that the shear flow stress of the work material decreases. It is also mentioned with the same explanation that the shear flow stress decreases with a decrease in rake angle and with an increase in cutting speed.

The shear strains based upon both flow region and conventional single shear plane theories were calculated for the S40C from the equation (9), and is shown in Fig. 8 in relation to microstructure.

It is obvious that the lamellar portion of pearlite has little affect on  $\gamma_2$ . Comparing  $\gamma_2$  with  $\gamma_0$ , the value of  $\frac{\gamma_0}{\gamma_2}$  decreases with an increase in carbon content and converges to 1.

**3.2.5. Comparison of lamellar pearlite and spheroidized pearlite**

Fig. 9 shows the result of cutting force and conventional shear angle in relation to feed and cutting speed. It was found that these values for spheroidized pearlite decreased in comparison with those for lamellar pearlite.

In this figure,  $\phi'$  shows the result of conventional shear angle for lamellar pearlite.

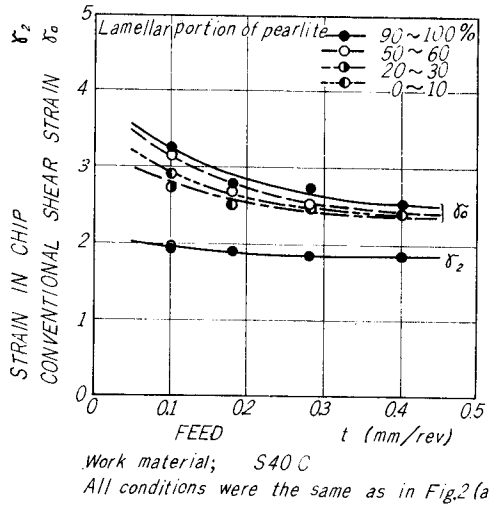


Fig. 8. Strain in chip and conventional shear strain of medium carbon steel in terms of feed.

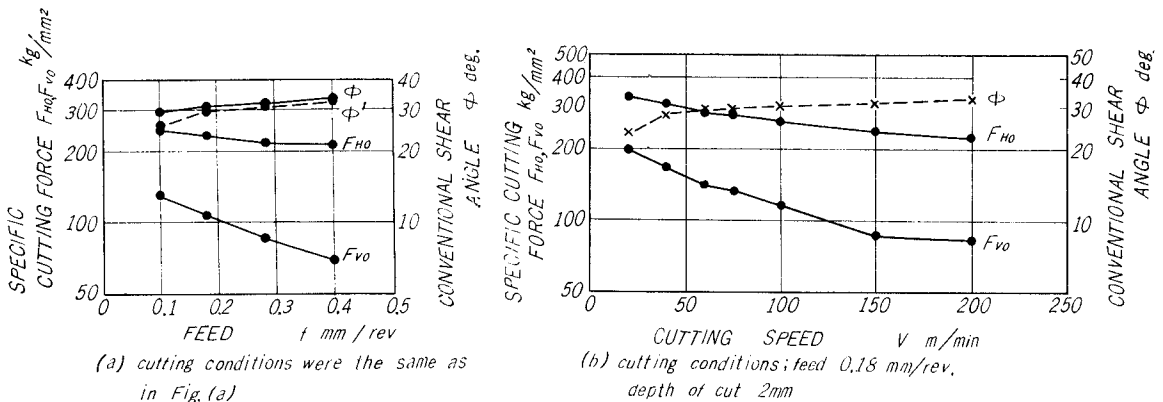


Fig. 9. Experimental results for spheroidized pearlite structure in terms of feed and cutting speed.

4. Machinability evaluation from the standpoint of tool life

4.1. Effect of microstructure

In this experiment, feed and depth of cut were kept constant, i.e., 0.28 mm/rev. and 1 mm, respectively, and the cutting speed was varied.

Tool life data are shown in Fig. 10 (a)-(c). In this figure, (a), (b) and (c) show tool life data in dry cutting for high, medium, and low carbon steels, respectively. The criterion of tool life in this case is a flank wear of 0.3 mm or a crater wear of 0.05 mm.

The Taylor tool life equation which shows the relationship between cutting speed  $V$  in m/min. and tool life  $T$  in min. is given by the following equation :

$$VT^n = C,$$

where  $C$  and  $n$  constants.

The Taylor tool life equations and cutting speed of 60 min. tool life for the materials tested above are given in Table 3.

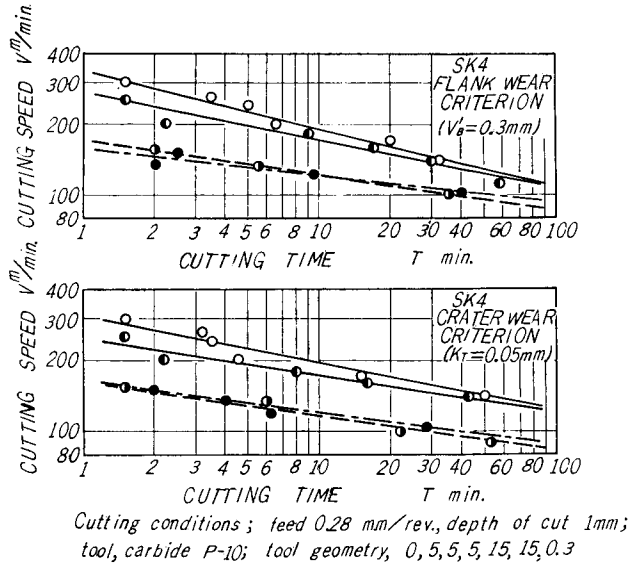


Fig. 10(a). Tool life plots for high carbon steel (SK4) of different microstructure.

Signature : ● lamellar portion of pearlite 90~100%  
 ○ " 50~ 60  
 ◐ " 20~ 30  
 ● " 0~ 10

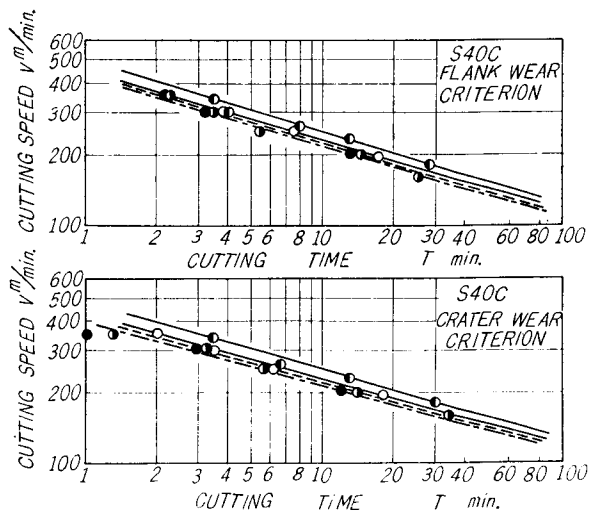


Fig. 10(b). Tool life plots for medium carbon steel (S40C) of different microstructure.

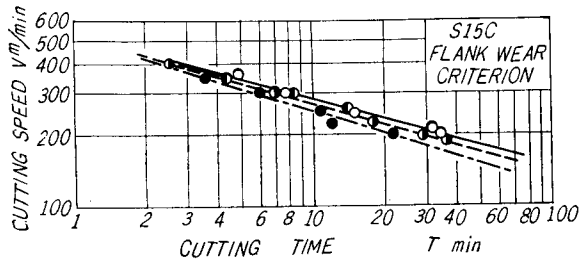


Fig. 10(c). Tool life plots for low carbon steel (S15C) of different microstructure.

Table 3. The Taylor tool life equations and cutting speed of 60 min. tool life for the material tested

Work material	Lamellar portion of pearlite (%)	Tool life equation		$V_{60}$ m/min	
		F	C	F	C
SK 4	90~100	$VT^{0.21}=275$	$VT^{0.16}=245$	119	130
	50~60	$VT^{0.24}=315$	$VT^{0.20}=300$	122	134
	20~30	$VT^{0.15}=175$	$VT^{0.16}=165$	95	90
	0~10	$VT^{0.13}=160$	$VT^{0.14}=160$	97	92
S 40 C	90~100	$VT^{0.31}=480$	$VT^{0.26}=460$	145	145
	50~60	$VT^{0.29}=440$	$VT^{0.26}=420$	135	137
	20~30	$VT^{0.31}=430$	$VT^{0.28}=400$	130	135
	0~10	$VT^{0.31}=425$	$VT^{0.30}=390$	130	130
S 15 C	90~100	$VT^{0.29}=530$	—	170	—
	50~60	$VT^{0.29}=530$	—	170	—
	20~30	$VT^{0.27}=520$	—	160	—
	0~10	$VT^{0.30}=520$	—	142	—

F; flank wear criterion ( $V_B'=0.3$  mm)  
 C; crater wear criterion ( $K_F=0.05$  mm)

(a) In the case of high carbon steel

It is evident that tool life for high carbon steel varies considerably with different pearlitic microstructure. This depends upon whether the lamellar portion of pearlite is above or below 50%. The maximum value of tool life was obtained when the lamellar portion of pearlite was about 50-60%.

The value of  $n$  in the tool life equation differs considerably in high speeds. Because hardness of the carbide in carbon steels (this carbide is considered to promote the tool wear) decreases and shear flow stress of the work ma-

terial decreases with an increase of lamination of the portion of pearlite in steels.

Brinell hardness of the portion of pearlite varied with the lamellar portion and showed a minimum value at the 50-60% lamination of pearlitic structure as shown in Table 2.

Shear stress on the shear plane in cutting calculated from experimental data as follows: 83 kg/mm<sup>2</sup> for 0-10% lamellar portion, 86 kg/mm<sup>2</sup> for 20-30% lamellar portion, 75 kg/mm<sup>2</sup> for lamellar portion 50-60%, and 78 kg/mm<sup>2</sup> for lamellar portion of 90-100%. It is evident from this result that shear stress on the shear plane shows the lowest value for lamellar portion of pearlite of 50-60%. This value relates with a maximum value of tool life.

Generally, it is difficult to machine the lamellar pearlitic materials compared with spheroidized pearlite materials. As discussed later, this fact is true. For the lamellar pearlitic materials, tool life can be improved considerably controlling the lamellar pearlite.

(b) In the case of medium carbon steel

Tool life for medium carbon steel is in the order of lamellar pearlite of 90-100% (best), 50-60%, 20-30% and 0-10%.

This is explained similarly in the case of SK4 as mentioned previously.

Table 4 shows the measured values of Brinell hardness for the parts of

Table 4. Measured values of Brinell hardness for the parts of pearlite and ferrite and calculated values of shear stress (S40 C)

Lamellar portion of pearlite (%)	0~10	20~30	50~60	90~100
Hardness of ferrite	200	192	147	147
Hardness of pearlite	279	274	267	255
Shear stress (kg/mm <sup>2</sup> )	67.5	70	68	65.5

pearlite and ferrite and shear stress on the shear plane.

It is evident from this that hardness of carbide and shear stress on the shear plane decrease with an increase in the lamellar portion of pearlite.

(c) In the case of low carbon steel

An adequate criterion of tool life when cutting low carbon steels is flank wear because of the small amount of crater wear. A tool life diagram determined from the standpoint of crater wear could not be obtained in this experiment.

Tool life showed a little difference with the variation of the lamellar portion of pearlite.

Observed and calculated results on Brinell hardness of pearlite and ferrite and shear stress on the shear plane in cutting are shown in Table 5.

Table 5. Measured values of Brinell hardness for the parts of pearlite and ferrite and calculated values of shear stress (S 15 C)

Lamellar portion of pearlite (%)	0~10	20~30	50~60	90~100
Hardness of ferrite	112	116	123	144
Hardness of pearlite	223	224	244	209
Shear stress (kg/mm <sup>2</sup> )	51.5	51	51	50.5

It is evident from this table that there is little difference on tool life for materials varying in lamellar portion of pearlite from 90-100% to 0-10% in spite of difference in Brinell hardness.

#### 4.2. Effects of grain size and nonmetallic constituents

Effects of grain size and nonmetallic constituents in steels on machinability has been stated in several papers<sup>5)</sup>. In this section, the authors will discuss the effects of grain size and nonmetallic constituents in carbon steel.

Table 6 shows the measured values of grain size accompanied with the

Table 6. Grain size for the materials tested

Lamellar portion of pearlite	Measuremental method	0~10	20~30	50~60	90~100
SK 4	Gf	6.0	6.0	4.2	4.7
S 40 C	FG <sub>c</sub> -P	7.5	7.7	7.5	7.2
S 15 C	FG <sub>c</sub> -P	7.2	7.0	6.8	7.0

variation of microstructure of SK4, S40C and S15C.

Grain size in high carbon steels depend upon the lamellar portion of pearlite, especially, a considerable difference shows for lamellar portion of 50-60% compared with that for lamellar portion below 20-30%. It appears from this result that materials with coarse grain size can be machined more easily than materials with fine grain size.

In other words, grain size in high carbon steels appears effective as a secondary factor.

On the other hand, it has less affect on the S40C and the S15C materials.

Regarding the nonmetallic constituents tested, it was found that nonmetallic constituents of A and C classes indicated by the JIS method are included in the steels tested. A class nonmetallic constituents have the following property : Stickness deformation is easily done at high temperature and the inclusion

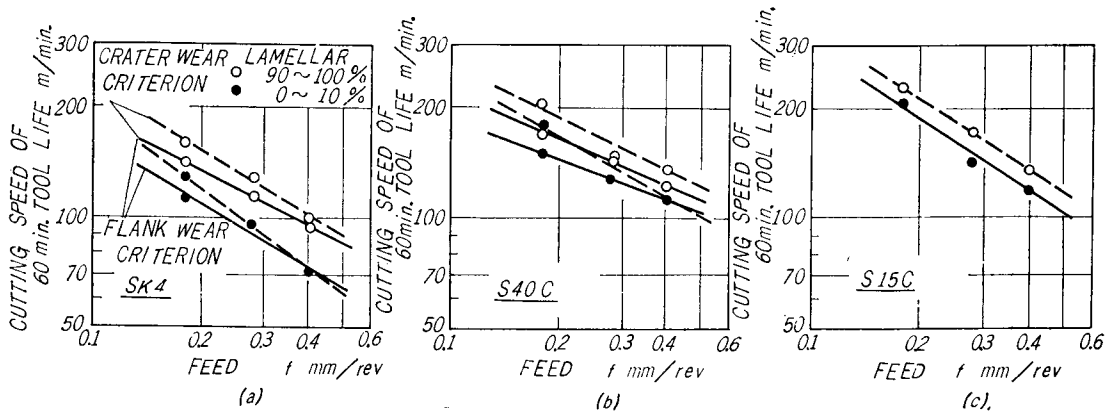


particle is lengthened towards the cutting direction. For C class, nonmetallic constituent FeO, MnO, etc. are included in the form of pieces.

It appears from the experimental results that nonmetallic inclusions in these materials have no effect on tool life.

#### 4.3. Effect of feed

The effect of feed on tool life is shown in Fig. 11. Materials of 6 kinds,



Cutting conditions were the same as Fig. 10

Fig. 11. Effect of feed on tool life.

that is, high, medium, and low carbon steels with lamellar portion of pearlite of 90-100% and 0-10% were tested.

It was found that for these materials the tool life is determined by flank wear below 0.40 mm/rev. and by crater wear for feed above 0.40 mm/rev.

#### 4.4. Comparison of tool life for materials with lamellar pearlite and with spheroidized pearlite

High carbon materials including carbon above 0.55% shows the shortest tool life due to high hardness of carbide.

For economical cutting, it is necessary to increase the stiffness of materials by lowering the hardness of the carbide.

In the section, the authors investigated machinability of carbon steel containing spheroidized pearlite and compared it with machinability of carbon steel containing lamellar pearlite. The effect of feed on tool life is shown in Fig. 12.

It was found that for materials with spheroidized pearlite the tool life is determined by flank wear for feed above 0.25 mm/rev. and by crater wear for feed below 0.25 mm/rev.

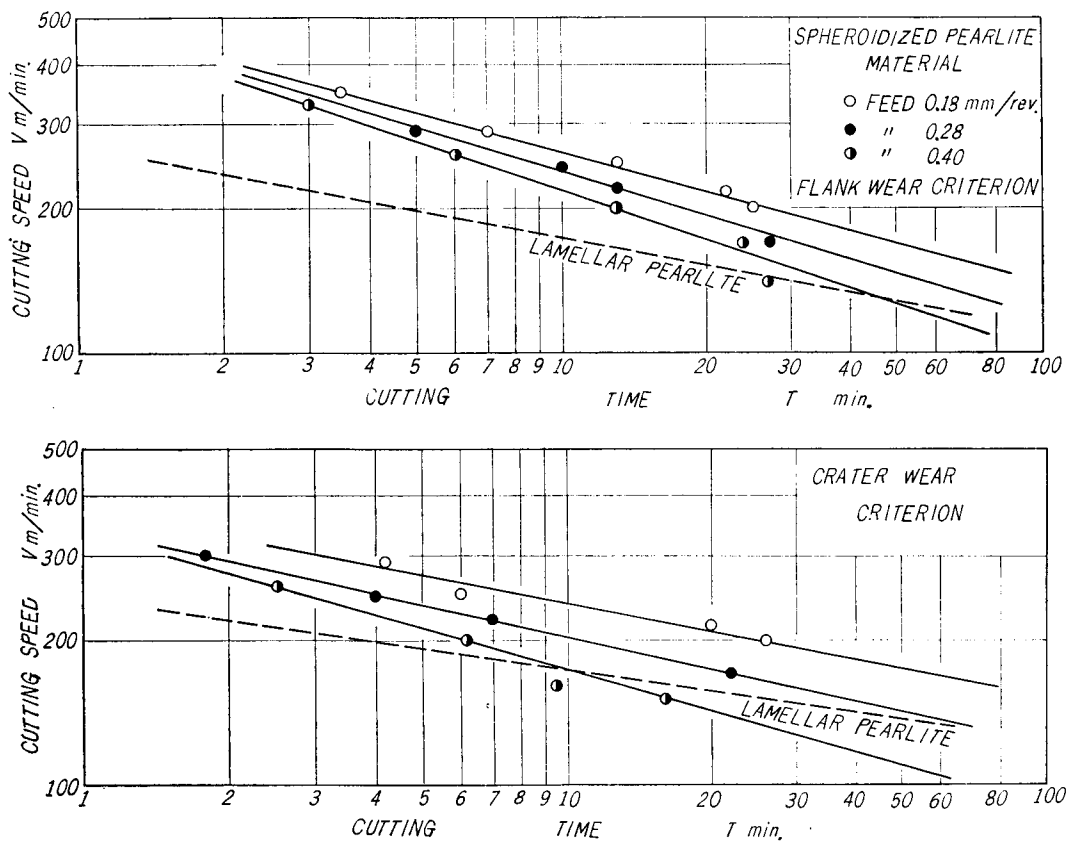


Fig. 12. Tool life plots of spheroidized pearlite material for feed.  
 Cutting conditions; depth of cut 1 mm, tool geometry, 0, 5, 5, 5, 15, 15, 0.3 mm;  
 fluid none: The criterion of tool life  $V_B' = 0.3 \text{ mm}$   $K_T = 0.05 \text{ mm}$

The American Air Force Machinability Report<sup>6)</sup> state that allowable cutting speed for materials containing spheroidized pearlite increases by about 70-80% for the same cutting volume (200 in<sup>3</sup>) compared with materials containing lamellar pearlite.

In this experiment, spheroidized pearlite was found to increase tool life more than lamellar pearlite, though lamellar pearlite contains carbon of 0.99% and spheroidized pearlite contains carbon of 1.32%.

Because of this reason spheroidized pearlite is softer than lamellar pearlite and so the cutting process is smoother.

### 5. Machinability evaluation from the standpoint of surface finish

#### 5.1. Effect of microstructure on surface finish

The effect of microstructure was investigated with a carbide tool P-10 (ISO)

from the standpoint of surface finish.

In this experiment, depth of cut was kept constant, i.e., 0.5 mm, and cutting speed and feed were varied: 10-220 m/min. for cutting speed and 0.06, 0.18, and 0.28 mm/rev. for feed.

Fig. 13 shows the experimental results on surface roughness. It is well

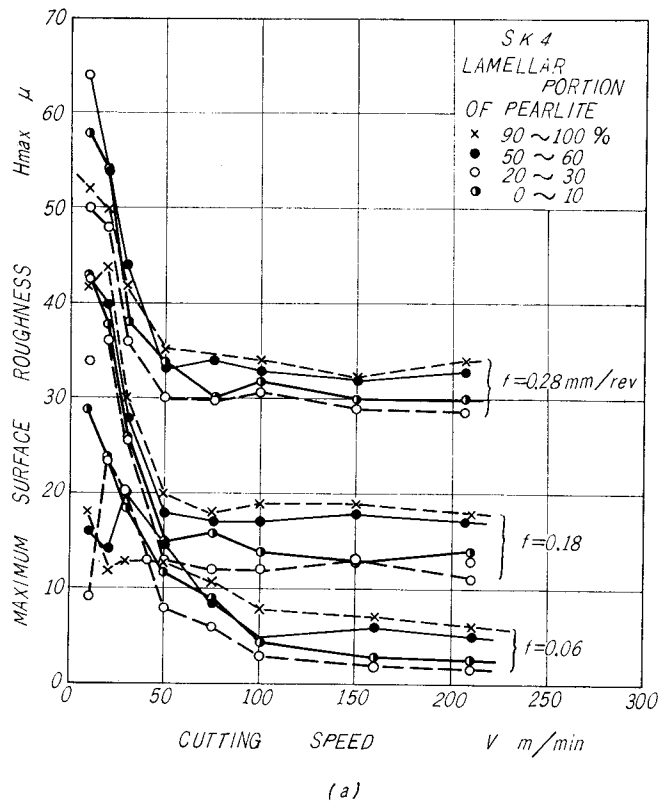
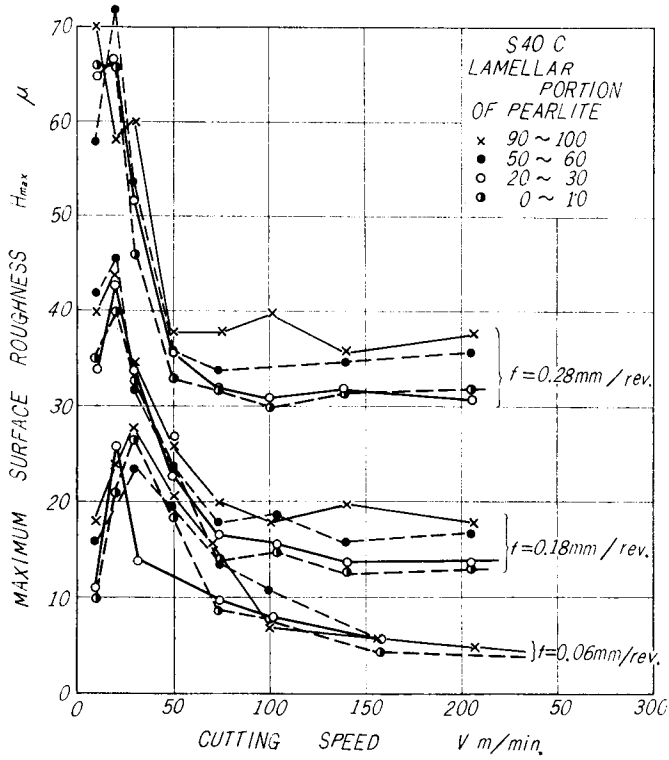


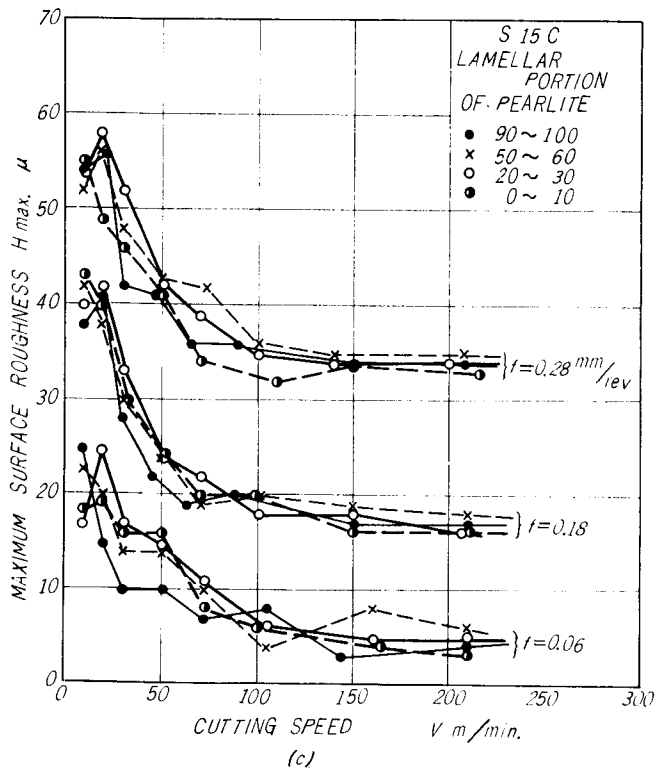
Fig. 13. Variation of maximum surface roughness for work materials with various lamellar portion of pearlite.  
Cutting conditions; depth of cut 0.5 mm; fluid, none;  
tool geometry, 0, 5, 5, 5, 15, 15, 0.3 mm.

known that surface roughness increases when a built-up edge occurs on the cutting edge at low and medium speeds. On the other hand, the degree of surface roughness is also affected considerably by the microstructure of the material.

In the case of high carbon steels, surface finish was in the order of 20-30%, 0-10%, 90-100% and 50-60% for lamellar pearlite. It was found that a considerable difference for surface finish was observed for lamellar portion of pearlite of above and below 50-60%.



(b)  
Fig. 13.



(c)  
Fig. 13.

In the case of medium carbon steels, surface finish was best for lamellar pearlite of 0-10% and was worst for lamellar pearlite of 90-100%.

In the case of low carbon steels, surface finish was worst for lamellar pearlite 90-100% but other materials showed no difference.

### 5.2. Effect of feed

Relationship between surface finish and feed is shown in Fig. 14. Surface roughness increased with an increase in feed a considerable effect was shown by microstructure on surface finish.

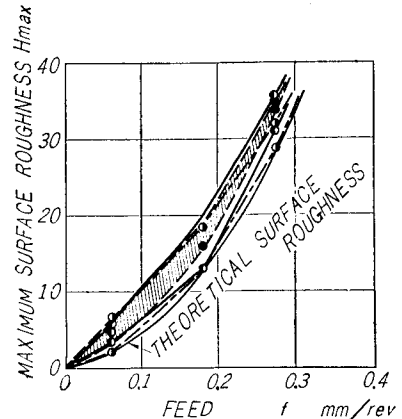


Fig. 14. Effect of feed on maximum surface roughness cutting speed, 150 m/min. All other conditions were the same as Fig. 13.

## 6. Conclusions

The above experiments and discussion lead to the following conclusions.

1. The cutting mechanism for carbon steels containing lamellar and spheroidized pearlite was analysed based upon the flow region concept.

The effects of feed, side rake angle, and microstructure on the cutting process were discussed.

It was found that the cutting mechanism for high, medium, and low carbon steels depends on microstructure.

2. Effect of lamellar portion of pearlite on tool life was investigated in detail and compared with effect of spheroidized pearlite.

Grain size and nonmetallic constituents also discussed on tool life. Grain size was found to effect on tool life.

3. Microstructure of lamellar pearlite affects the surface finish. Surface roughness was small for lamellar pearlite of 20-30% in high carbon steels.

## Reference

- 1) K. Okushima and others; Trans. JSME **21**, 110 (1955) p. 709-711.
- 2) K. Okushima and K. Hitomi; Trans. JSME **25**, 150 (1959) p. 54-60.
- 3) K. Okushima and K. Hitomi; Trans. ASME Series B, Journal of Engineering for Industry, No. 4, 1961, p. 545-556.
- 4) K. Okushima and K. Iwata; Memoirs of Faculty of Engineering, Kyoto University, Vol. XXIV, Part 1, January 1962, p. 1-21.
- 5) For Example, Woldman and Gibbons; Machinability and machining of Metals (1951).
- 6) United State Air Force Machinability Report Vol. 1, 1950, Vol. 2, 1951.